

## Scanning-tunneling-microscopy studies of disilane adsorption and pyrolytic growth on Si(100)-(2×1)

D.-S. Lin, E. S. Hirschorn, and T.-C. Chiang

*Department of Physics and Materials Research Laboratory, University of Illinois at Urbana-Champaign, Urbana, Illinois 61801*

R. Tsu, D. Lubben, and J. E. Greene

*Department of Materials Science, Coordinated Science Laboratory, University of Illinois at Urbana-Champaign, Urbana, Illinois 61801  
and Materials Research Laboratory, University of Illinois at Urbana-Champaign, Urbana, Illinois 61801*

(Received 19 August 1991)

Scanning tunneling microscopy has been employed to study the adsorption of disilane ( $\text{Si}_2\text{H}_6$ ) and pyrolytic growth on Si(100)-(2×1) at various temperatures. Room-temperature exposures result in a random distribution of dissociation fragments on the surface. Formation of anisotropic monohydride islands and denuded zones as well as island coarsening is observed at higher temperatures. The results are strikingly similar to those reported for growth by molecular-beam epitaxy using pure Si, even though different surface reactions are involved in these two growth processes.

### I. INTRODUCTION

Chemical vapor deposition (CVD) has been employed in semiconductor crystal growth for years. For the growth of epitaxial Si layers, CVD has several advantages compared to Si molecular-beam epitaxy (MBE), which suffers from low dopant-incorporation probabilities and high dopant-surface-segregation rates.<sup>1,2</sup> Both silane ( $\text{SiH}_4$ ) and disilane ( $\text{Si}_2\text{H}_6$ ) have been used in Si CVD. Of these two gases, disilane has orders-of-magnitude higher reactivities due to a lower decomposition activation energy, and therefore epitaxial film growth can be achieved at a much lower substrate temperature.<sup>3-6</sup> The lower decomposition activation energy of disilane is related to the lower bond energy for Si—Si than for Si—H in the  $\text{Si}_2\text{H}_6$  molecule. The dissociative chemisorption of disilane on Si(100) is initiated by cleavage of this Si—Si bond to form two silyl ( $\text{SiH}_3$ ) radicals on two adjacent dangling-bond sites.<sup>3-5</sup> The silyl radicals can further decompose to form silylene ( $\text{SiH}_2$ ) and H, and the resulting surface can exhibit a mixture of Si dangling bonds and mono-, di-, and trihydride species depending upon the experimental conditions.<sup>3,4,6</sup> With increasing substrate temperatures, further pyrolytic reactions take place on the surface, and hydrogen desorption is observed to occur in two stages.<sup>3,4,6,7</sup> The higher hydrides decompose to form monohydride at about 350°C–400°C. The monohydride decomposes at about 500°C–550°C, and the resulting surface is a clean Si(100)-(2×1).

In this paper, we present the results of a scanning-tunneling-microscopy (STM) investigation of the essential steps involved in the CVD growth of Si using disilane. We have observed the formation of anisotropic monohydride islands and denuded zones as well as island coarsening. The results bear striking similarities to the growth of Si by conventional Si MBE,<sup>8-13</sup> even though the presence of terminating hydrogen on the surface during CVD growth gives rise to different surface reactions.

### II. EXPERIMENTAL PROCEDURE

The experiment was carried out in a vacuum chamber having a base pressure in the  $10^{-11}$ -torr range. The microscope has been described in a previous publication.<sup>14</sup> All pictures were taken with a tunneling current of 0.3–0.35 nA. The Si substrates used were prepared from commercial *n*-type, nominally on-axis, Si(100) wafers. The substrate size was  $0.4 \times 1.2 \times 0.04$  cm<sup>3</sup>. Each substrate was degreased before insertion into the vacuum chamber. Substrate cleaning involved outgassing at about 600°C for many hours followed by heating to ~1100°C for about 10 s. Heating of the sample was accomplished by passing a current through the sample. This procedure consistently produced surfaces exhibiting sharp (2×1) diffraction patterns with no contamination as determined by photoemission and Auger spectroscopy. The temperature of the sample as a function of heating power was calibrated by attaching a small thermocouple to the center of the front face of an identical test sample. Disilane was introduced into the chamber through a precision leak valve. The dosing pressure, calibrated by an ion gauge and monitored using the ion pump current, was in the range of  $10^{-8}$ – $10^{-7}$  torr. The pressure readings were corrected by the ion gauge sensitivity to disilane (2.4 relative to air).<sup>15</sup> For dosing at elevated substrate temperatures, the heating current was turned off one minute after the termination of the exposure and the sample was allowed to cool down to near room temperature before STM imaging.

### III. RESULTS AND DISCUSSION

Figure 1(a) shows a typical STM picture of a starting clean Si(100)-(2×1) surface. The scan size is about  $2000 \times 3800$  Å<sup>2</sup>. The individual (2×1) dimers cannot be seen at this scale.<sup>8-13</sup> The primary features seen in the picture are single atomic steps. This picture has been

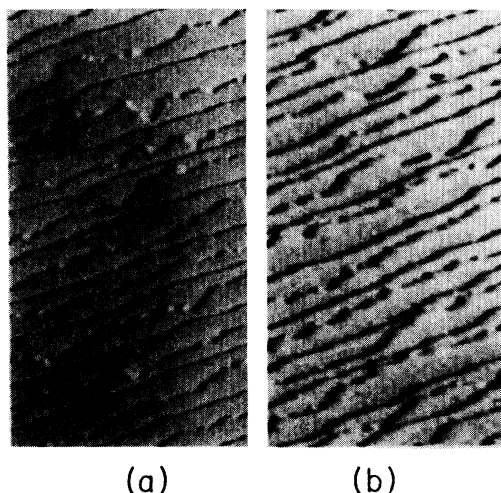


FIG. 1. STM images over an area of  $2000 \times 3800 \text{ \AA}^2$  for (a) clean Si(100)-(2  $\times$  1) and (b) the same sample after CVD growth at 550°C using disilane for an exposure of 90 L. The sample bias is  $-2 \text{ V}$ .

filtered to remove the low-spatial-frequency components, and resembles a landscape with light illumination from the western sky. The steps separating flat terraces are alternately relatively smooth and rough corresponding to type-*A* and -*B* steps, respectively.<sup>16</sup> For a type-*A* (-*B*) step, the dimer bond direction in the upper terrace is perpendicular (parallel) to the step edge. From the average spacing between neighboring steps, a miscut of about  $0.4^\circ$  is deduced for this particular surface corresponding to an average terrace width of  $\sim 200 \text{ \AA}$ , although the wafer used is nominally on axis. All of the STM pictures to be presented below have been filtered in a similar fashion. The miscut may be different for different samples.

Exposing clean Si(100)-(2 $\times$ 1) to disilane at room temperature results in randomly distributed dissociation fragments on the surface, which show no preference for areas near steps or defects. Apparently, the fragments do not have sufficient mobility on the surface to form islands or cluster or to migrate and attach to steps. The fully saturated surface is disordered, in agreement with Ref. 7.

At higher adsorption temperatures, ordering of the fragments is observed. Figures 2(a) and 2(b) show STM images of a sample after a 1.2-L disilane exposure at 350°C. These two pictures, acquired simultaneously over the same area for sample bias voltages of  $+2$  and  $-1.3 \text{ V}$ , respectively, show the spatial distribution of unoccupied and occupied states near the Fermi level. The scan size is about  $100 \times 140 \text{ \AA}^2$ . At the chosen substrate temperature, the higher hydrides are converted to stable monohydride. Here, one observes that one-dimensional islands are formed on the (2 $\times$ 1) dimer surface. The long axis of each island is orthogonal to the underlying dimer rows, and corresponds to the expected dimer row direction for Si growth. Since monohydride is known to form dimer configurations on Si,<sup>7,17,18</sup> we can attribute these islands to monohydride dimer rows. A monohydride dimer row has the same configuration as a Si dimer row except that the dimer dangling bonds for the Si dimer row

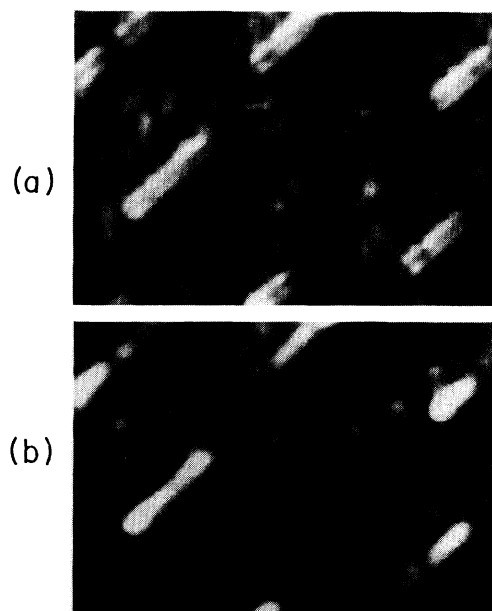


FIG. 2. Dual-voltage images of Si(100) dosed with 1.2-L disilane at 350°C. Pictures (a) and (b) are taken with a sample bias of  $+2$  and  $-1.3 \text{ V}$ , respectively, over the same area ( $100 \times 140 \text{ \AA}^2$ ).

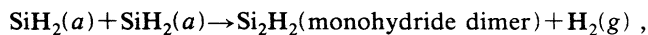
are replaced by Si—H bonds. The islands in the unoccupied-state image, Fig. 2(a), show apparent splitting along the long axis, while the substrate Si dimer rows do not show such splitting. This can be attributed to the different electronic properties of the monohydride surface compared to clean Si(100)-(2 $\times$ 1). The termination of the dimer dangling bonds on Si(100)-(2 $\times$ 1) by hydrogen to form monohydride gives rise to a broad H-derived  $\sigma^*$  state located at about 1 eV above the Fermi energy.<sup>18–20</sup> The resulting spatial localization of the unoccupied states near the two hydrogen atoms of a dimer causes the dimer image to split.<sup>18</sup>

From Fig. 2 and other similar micrographs, a monohydride island coverage of about 0.1 monolayer (ML) is deduced; here,  $1 \text{ ML} = 6.8 \times 10^{14} \text{ cm}^{-2}$  is the density of atoms in a Si(100) layer. This coverage is produced with a 1.2-L exposure, or a dose of  $3.2 \times 10^{14} \text{ cm}^{-2}$ . Taking into account the two Si atoms in each disilane molecule, the overall sticking probability for Si<sub>2</sub>H<sub>6</sub> is about 0.1 at 350°C under our experimental conditions. This is about the same as that for the Si(111)-(7 $\times$ 7) surface.<sup>5</sup>

As mentioned earlier, during the pyrolytic reaction on the surface SiH<sub>3</sub> radicals decompose into SiH<sub>2</sub> and H, and the H atom released can saturate a nearby dangling bond on the substrate surface:<sup>3,4,7</sup>



where (*a*) denotes an adsorbed configuration. The resulting dihydride radicals SiH<sub>2</sub> then diffuse and combine to form monohydride by releasing a H<sub>2</sub> molecule which leaves the surface:<sup>7</sup>



where (g) denotes the gas phase. To account for all of the hydrogen atoms, the part of the substrate surface in Fig. 2, not covered by the monohydride islands, should contain about 0.1 ML of terminating hydrogen. This is a very small coverage and the exposed substrate surface remains mostly free of hydrogen in agreement with the dual-voltage observation.

In the MBE growth of Si using a Si source, similar one-dimensional islands have been observed.<sup>8–13</sup> In that case, the islands are pure Si dimer rows, and Si adatoms are the diffusing species on the surface, which are to be compared with monohydride islands and SiH<sub>2</sub> diffusing species in the present case. Under similar experimental conditions (300°C–400°C growth temperatures and 0.1–0.2 ML coverages), Si MBE yielded anisotropic islands with aspect ratios in the range of 10–30.<sup>8</sup> In contrast, the present experiment shows a dimer chain length, averaged over many observations, of about 5 indicating a lower surface mobility which may be associated with the presence of H due to SiH<sub>3</sub> dissociation. Apart from this quantitative difference, the results are similar. The formation of anisotropic islands in the case of Si MBE has been discussed, and the main driving mechanism is thought to be a difference in accommodation probability between the sides and the ends of the dimer row during growth.<sup>9,10</sup> Apparently, a similar difference also exists in the present case.

Figure 3 shows a scan over a  $2000 \times 2000 \text{ \AA}^2$  area for a sample exposed to 7.5 L of disilane at 420°C. The sticking coefficient should not change much from 350° to 420°C,<sup>5</sup> so we expect a monohydride coverage about 0.6 ML based on a linear extrapolation of the results discussed earlier. The picture shows a high density of islands on terraces between alternating type-*A* and -*B* steps. To show details of these islands, we present in Fig. 4 dual-voltage images taken over an area of  $180 \times 180 \text{ \AA}^2$  in a terrace. Figures 4(a) and 4(b) are taken with a sample bias of +2 and -1.5 V, and correspond to images of the unoccupied and occupied states, respectively. The islands in these pictures, typically several dimer rows wide, are much larger than those seen in Fig. 2. The total island coverage is about 0.5 ML, quite close to the predicted value of 0.6 ML. The islands are still elongated along the dimer row direction, but the aspect ratio is smaller. This behavior is again qualitatively similar to the Si MBE growth results; namely, as the coverage and substrate temperature are increased, the islands become larger with a reduced aspect ratio.<sup>8–13</sup> Unoccupied-state images show that *all* of the dimer rows, both of the islands, and the substrate surface are split in the middle. [Splitting of the substrate surface dimer rows is difficult to see in Fig. 4(a) where the grey scale contrast was optimized for the islands.] This is the characteristic of a monohydride surface as mentioned earlier. Thus, the entire surface is terminated by hydrogen. This result is consistent with the reaction pathway described above; namely, there is enough hydrogen released by the decomposition of SiH<sub>3</sub> into SiH<sub>2</sub> to saturate all of the remaining dangling bonds.

Figure 5 shows growth at an even higher substrate

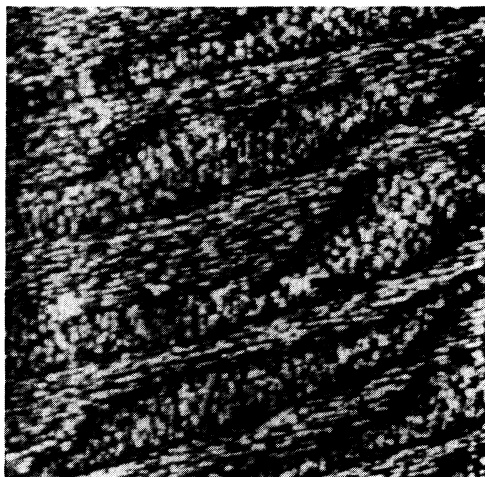


FIG. 3. A STM image over an area of  $2000 \times 2000 \text{ \AA}^2$  of Si(100) dosed with 7.5-L disilane at 420°C. The sample bias is -1.5 V.

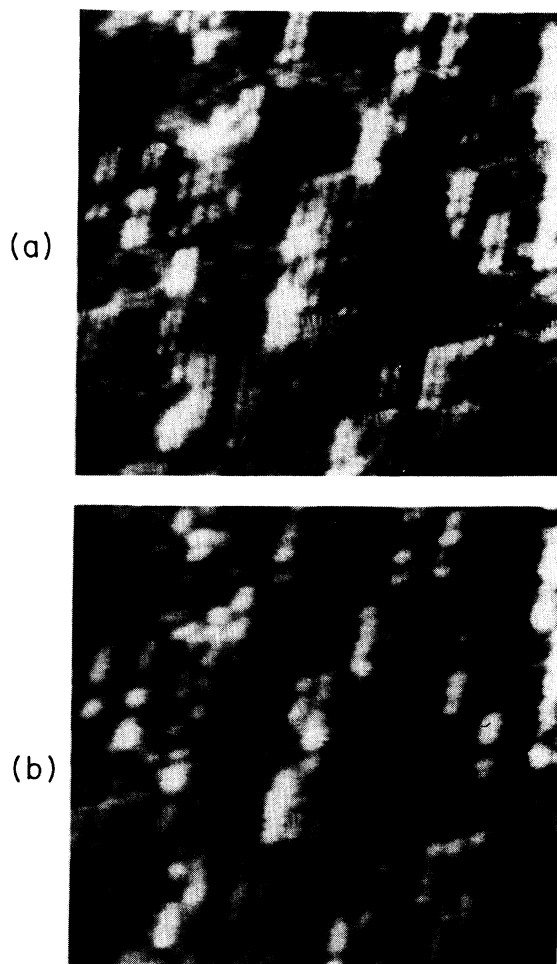


FIG. 4. Dual-voltage images of a  $180 \times 180 \text{ \AA}^2$  area within a flat terrace in Fig. 3. Pictures (a) and (b) are taken with a sample bias of +2 and -1.5 V, respectively.

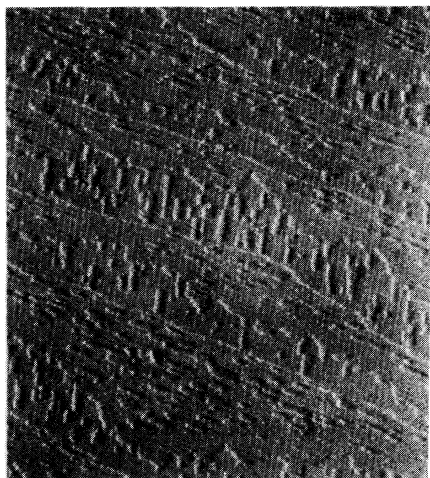


FIG. 5. A STM image over an area of  $3500 \times 4000 \text{ \AA}^2$  of Si(100) dosed with 3.3-L disilane at 455°C. The sample bias is  $-2 \text{ V}$ . Terrace heights increase from the lower left of the micrograph toward the upper right.

temperature of 455 C. This  $3500 \times 4000 \text{ \AA}^2$  picture is for a disilane exposure of 3.3 L; a coverage of about 0.3 ML is expected. Here again, one observes anisotropic islands on terraces between steps, and the islands are, on the average, larger than those seen in Fig. 3, even though the coverage here is less. This is due to edge boundary migration and island coarsening<sup>8-10</sup> reducing the total island boundary energy during deposition. Both effects, edge migration and coarsening, act to minimize kinetically controlled island growth anisotropy in favor of the formation of islands with a more nearly equilibrium shape. This implies that the system has a significantly higher mobility at this substrate temperature. Comparing this figure with Fig. 4, one also notices an important difference; namely, the region of terraces immediately neighboring type-B down steps exhibits a much reduced island density. This is the so-called denuded zone,<sup>10,13</sup> and is related to the anisotropy in diffusion along and across dimer rows. That is, in the up terrace dimer rows are perpendicular to the step and mobile species can reach and attach themselves to step edges, thus producing an island-depleted region. This does not occur on the down terrace where the dimer rows are parallel to step edges. As mentioned earlier, the accommodation probability is much higher at the ends of dimer rows than on the sides, so one can expect type-B steps to be a strong sink for diffusing radicals. Considering all of these effects, it is clear that denuded zones should form in regions immediately neighboring a type-B down step as seen in Fig. 5. The phenomena of island coarsening and denuded-zone formation have been observed for Si MBE growth,<sup>8-13</sup> and those results are very similar to the present observation.

Figure 1(b) shows a STM picture after an exposure of 90 L at 550 C. This picture was taken from the same sample from which the clean surface picture, Fig. 1(a), was obtained. The two pictures, taken under the same

bias and scan conditions, can be directly compared. At 550°C, the hydrogen is completely desorbed and multilayer growth occurs.<sup>2,4</sup> What one sees in Fig. 1(b) is a clean Si(100) surface, with terraces separated by type-A and -B steps, similar to Fig. 1(a). There is a subtle difference, however. The neighboring steps on the original surface are roughly equally spaced (ignoring the roughness of the type-B steps). The surface after multilayer growth exhibits a larger variation in step-to-step spacing. Some of the single steps appear to touch and combine to form segments of double steps, although single steps are known to be the more stable configuration for Si(100) with a small miscut.<sup>21</sup> This result is understandable as the multilayer growth occurs at a lower temperature than the initial annealing temperature, and the system is therefore farther away from the equilibrium configuration.

#### IV. SUMMARY

The initial adsorption of disilane at room temperature results in a random distribution of dissociation fragments, which is not correlated with defects or steps. The saturated surface is disordered. For higher adsorption temperatures (350°C–420°C), the fragments combine to form anisotropic monohydride islands elongated along the dimer row direction. The island growth anisotropy was found to be lower for disilane CVD growth than for Si MBE due, we believe, to adsorbed H from  $\text{SiH}_3$  decomposition decreasing Si radical surface diffusivity. The part of the surface not covered by the islands is also (partially) terminated by hydrogen derived from the decomposition of adsorbed  $\text{SiH}_3$ . Island coarsening and denuded-zone formation are observed at even higher substrate temperatures (455°C). Finally, at temperatures above the hydrogen desorption temperature, multilayer growth results in a smooth surface with somewhat uneven step distributions. All of these growth features are remarkably similar to those reported for Si MBE, even though different surface reactions are involved due to the presence of terminating hydrogen.

#### ACKNOWLEDGMENTS

This material is based upon work supported by the U.S. Department of Energy (Division of Materials Sciences, Office of Basic Energy Sciences), under Grant No. DEFG02-91ER45439 (T.C.C.), the Office of Naval Research, under Contract No. N00014-90-J-1241 (J.E.G.), and the Semiconductor Research Corporation (J.E.G.) Acknowledgment is also made to the Donors of the Petroleum Research Fund, administered by the American Chemical Society, and to the U.S. National Science Foundation (Grant No. DMR-89-19056) for partial personnel and equipment support (T.C.C.). We acknowledge the use of central facilities of the Materials Research Laboratory of the University of Illinois, which is supported by the U.S. Department of Energy (Division of Material Sciences, Office of Basic Energy Sciences), under Grant No. DEFG02-91ER45439, and the U.S. National Science Foundation under Grant No. DMR-89-20538.

- <sup>1</sup>M. A. Hasan, J. Knall, S. A. Barnett, J.-E. Sundgren, L. C. Markert, A. Rockett, and J. E. Greene, *J. Appl. Phys.* **65**, 172 (1989).
- <sup>2</sup>W.-X. Ni, M. A. Hasan, G. V. Hansson, J.-E. Sundgren, S. A. Barnett, L. C. Markert, and J. E. Greene, *Phys. Rev. B* **40**, 10449 (1989).
- <sup>3</sup>Y. Suda, D. Lubben, T. Motooka, and J. Greene, *J. Vac. Sci. Technol. A* **8**, 61 (1990).
- <sup>4</sup>D. Lubben, R. Tsu, T. R. Bramblett, and J. Greene, *J. Vac. Sci. Technol. A* **9**, 3003 (1991).
- <sup>5</sup>S. M. Gates, *Surf. Sci.* **195**, 307 (1988).
- <sup>6</sup>Y. Suda, D. Lubben, T. Motooka, and J. Greene, *J. Vac. Sci. Technol. B* **7**, 1171 (1989).
- <sup>7</sup>J. J. Boland, *Phys. Rev. B* **44**, 1383 (1991).
- <sup>8</sup>R. J. Hamers, U. K. Kohler, and J. E. Demuth, *J. Vac. Sci. Technol. A* **8**, 195 (1990); *Ultramicroscopy* **31**, 10 (1989).
- <sup>9</sup>Y. W. Mo, B. S. Swartzentruber, R. Kariotis, M. B. Webb, and M. G. Lagally, *Phys. Rev. Lett.* **63**, 2393 (1989).
- <sup>10</sup>Y. W. Mo, R. Kariotis, B. S. Swartzentruber, M. B. Webb, and M. G. Lagally, *J. Vac. Sci. Technol. A* **8**, 201 (1990).
- <sup>11</sup>Y. W. Mo, J. Kleiner, M. B. Webb, and M. G. Lagally, *Phys. Rev. Lett.* **66**, 1998 (1991).
- <sup>12</sup>Y.-W. Mo, R. Kariotis, D. E. Savage, and M. G. Lagally, *Surf. Sci.* **219**, L551 (1989).
- <sup>13</sup>Y.-W. Mo, Ph.D. thesis, University of Wisconsin–Madison, 1991.
- <sup>14</sup>F. M. Leibsle, A. Samsavar, and T.-C. Chiang, *Phys. Rev. B* **38**, 5780 (1988).
- <sup>15</sup>R. Imbihl, J. E. Demuth, S. M. Gates, and B. A. Scott, *Phys. Rev. B* **39**, 5222 (1989).
- <sup>16</sup>D. J. Chadi, *Phys. Rev. Lett.* **59**, 1691 (1987).
- <sup>17</sup>T. Sakurai and H. D. Hagstrum, *Phys. Rev. B* **14**, 1593 (1976).
- <sup>18</sup>J. J. Boland, *Phys. Rev. Lett.* **65**, 3325 (1990).
- <sup>19</sup>S. Ciraci, R. Butz, E. M. Oellig, and H. Wagner, *Phys. Rev. B* **30**, 711 (1984).
- <sup>20</sup>R. J. Hamers, P. Avouris, and F. Bozso, *Phys. Rev. Lett.* **59**, 2071 (1987).
- <sup>21</sup>T. W. Poon, S. Yip, P. S. Ho, and F. F. Abraham, *Phys. Rev. Lett.* **65**, 2161 (1990).

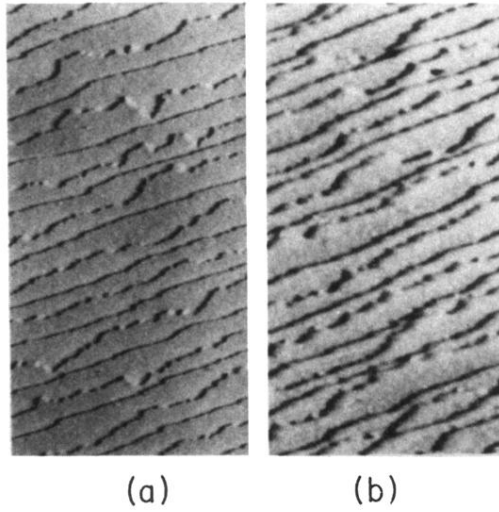


FIG. 1. STM images over an area of  $2000 \times 3800 \text{ \AA}^2$  for (a) clean Si(100)-(2  $\times$  1) and (b) the same sample after CVD growth at 550°C using disilane for an exposure of 90 L. The sample bias is  $-2 \text{ V}$ .

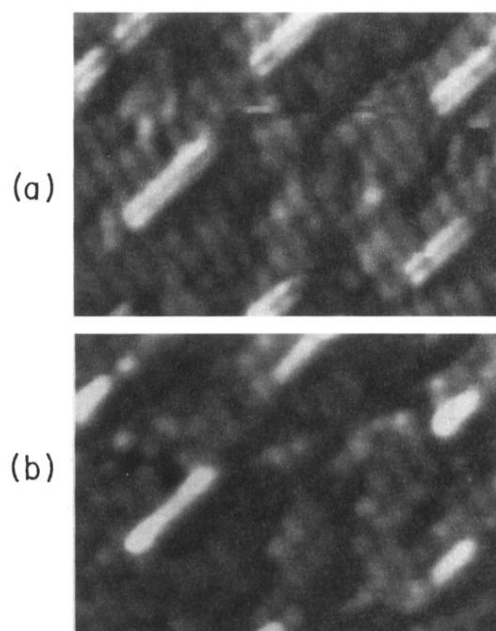


FIG. 2. Dual-voltage images of Si(100) dosed with 1.2-L disilane at 350°C. Pictures (a) and (b) are taken with a sample bias of +2 and -1.3 V, respectively, over the same area ( $100 \times 140 \text{ \AA}^2$ ).

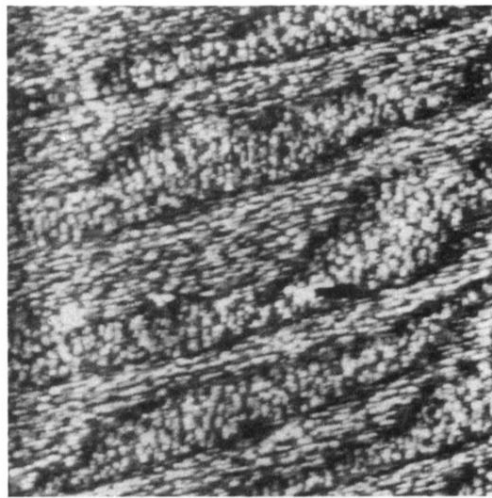


FIG. 3. A STM image over an area of  $2000 \times 2000 \text{ \AA}^2$  of SI(100) dosed with 7.5-L disilane at  $420^\circ\text{C}$ . The sample bias is  $-1.5 \text{ V}$ .



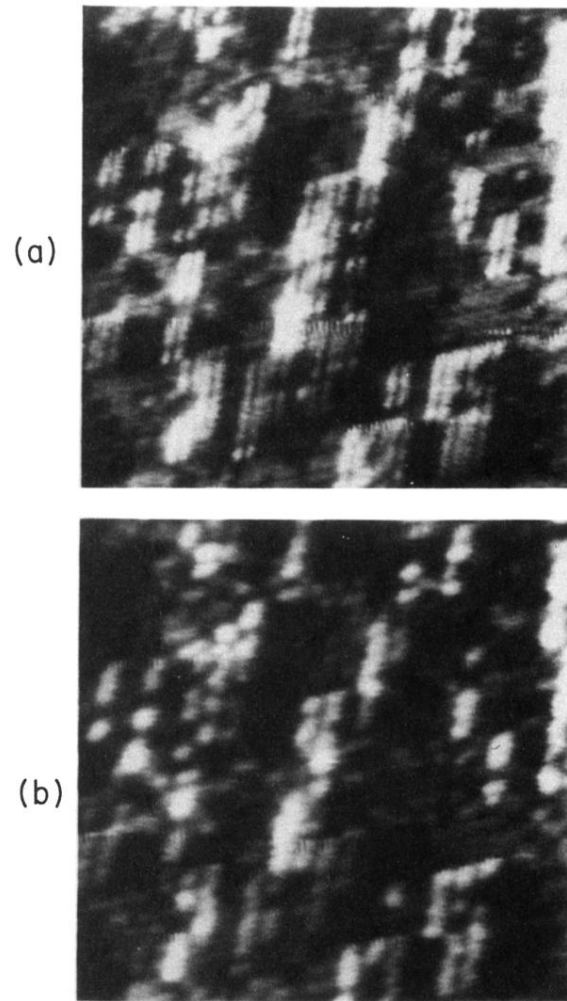


FIG. 4. Dual-voltage images of a  $180 \times 180 \text{ \AA}^2$  area within a flat terrace in Fig. 3. Pictures (a) and (b) are taken with a sample bias of +2 and  $-1.5 \text{ V}$ , respectively.



FIG. 5. A STM image over an area of  $3500 \times 4000 \text{ \AA}^2$  of Si(100) dosed with 3.3-L disilane at  $455^\circ\text{C}$ . The sample bias is  $-2 \text{ V}$ . Terrace heights increase from the lower left of the micrograph toward the upper right.